

A note on low drag bodies

Paper given at the XI OSTIV Congress, Lesyno, Poland, June 1968

By Francisco Leme Galvao, Aer. Ing., Design Dept. S. C. Aeronáutica Neiva Lt, Brasil

1. Summary

This note suggests a straightforward method for—obtaining low drag three-dimensional bodies from tabulated low drag airfoil ordinates.

2. Introduction

Although a considerable amount of theoretical and experimental work has already been done on low drag wing sections, the same is not true in subsonic flow, for three-dimensional bodies.

The available data are scarce and many of them date from the lighter-than-air period, with few modern works on the subject, that have been overlooked by many subsonic aircraft designers.

However in glider design, fuselage aerodynamics is

gaining more and more importance as glider speeds are moving up.

Many sailplanes have fuselage shapes whose projections (plan and elevation) are similar to low drag airfoil contours. However a simple study of potential flow theory, points out that different results are obtained with the same shape, in two- or three-dimensional flows.

A striking example of that, is the comparison of the potential flow past a cylinder and past a sphere (see fig. 1) the difference being greater if pressure gradients rather than pressure distributions, are compared (ref. 1).

In reference 2 the potential flow past an airfoil shaped body of revolution is obtained by means of conformal mapping transformation of flow past a sphere and computed values of pressure are less than for the corresponding two-dimensional case.

So, such airfoil shaped bodies, may not provide negative pressure gradients of sufficient magnitude in the forebody

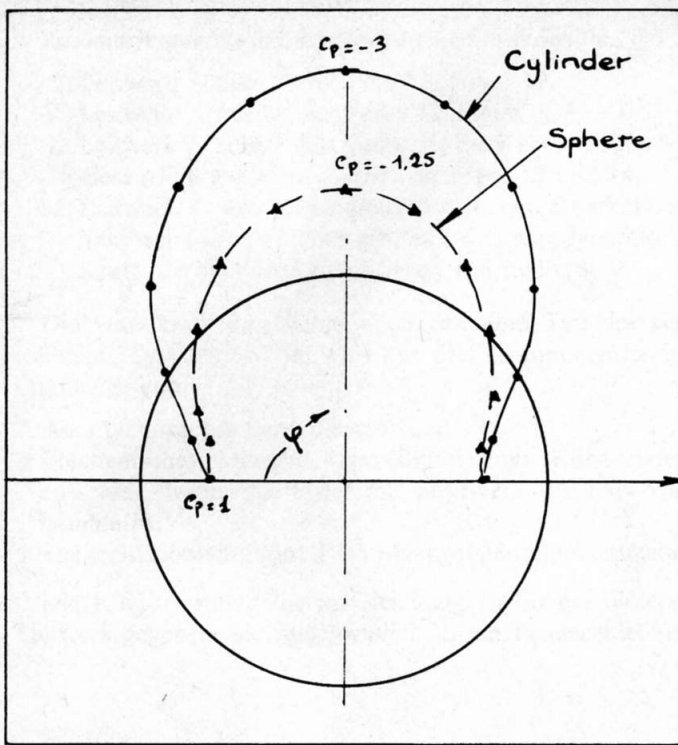


Fig. 1 - Pressure distribution of potential flow past a cylinder and a sphere - Ref. 1.

to maintain the laminar condition of the flow at Reynolds Numbers such as those of glider fuselages (R.N. about 6 to 13×10^6).

The well-known method of superposing sources and sinks to a parallel flow may also be used to compute the velocity in the surface of a body of revolution with axis parallel to the main flow, the result being:

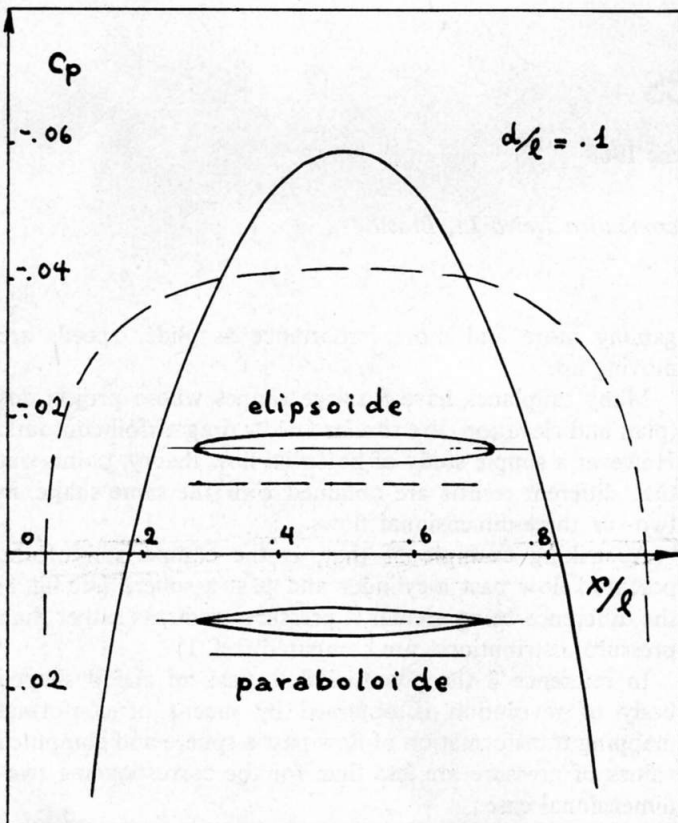


Fig. 2 - Pressure distribution along two elongated bodies of revolution in axial potential flow - Ref. 1

$$\vec{V} = \vec{U}_{\infty} + \vec{v} + \vec{w} \quad \text{where}$$

$$w(x) = U_{\infty} \frac{dR(x)}{dx}$$

$$V(x) = 0.25 \lim_{\epsilon \rightarrow 0} \left[2 \left(1 - \log \frac{\epsilon}{l} \right) \frac{d^2 R(x)^2}{dx^2} \right] + \int_0^{x-\epsilon} \frac{d(R(x')^2)}{dx'} \frac{dx'}{(x-x')^2} - \int_{x-\epsilon}^l \frac{d(R(x')^2)}{dx'} \frac{dx'}{(x-x')^2} + \frac{1}{2} \frac{d^2(R(x))}{dx^2} \log \frac{R}{l}$$

(ref. 1)

For simple geometrical forms, the solution is easily obtained and figure 2 illustrates the results for elliptic and parabolic elongated bodies of revolution ($d/l = 1$).

An interesting remark is that the three-dimensional parabolic case gives a pressure distribution closer to that of an elliptical two-dimensional cylinder than that obtained with a elliptical three-dimensional body!

3. The "three halves power law"

The two theoretical methods seen above would permit the design of a body with a prescribed pressure gradient law, for instance, that of a low drag airfoil.

However the amount of work required and mathematical knowledge is considerable and tabulated shapes are yet to be computed and tested.

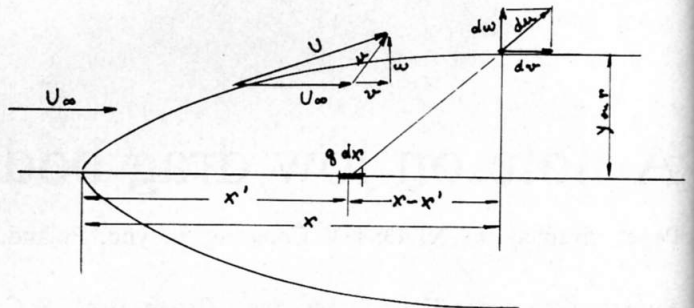


Fig. 3 - Velocity components of the text

So, if a simple relationship could be established, between two- and three-dimensional flows it would bring along the evident profits from using all the work already done in regard to wing sections.

Let us compare the potential solution for a two-dimensional airfoil with ordinate $y(x)$ with a three-dimensional body of revolution of radius $r(x)$, as obtained by the superposition of a uniform flow U_{∞} , and a line of two- and three-dimensional sources and sinks of intensity $q_2(x)$ and $q_3(x)$ (see fig. 3).

The velocity increase caused by a source or sink element $q dy$ is in each case:

$$du_2 = \frac{q_2 dx'}{2\pi [y^2 + (x-x')^2]^{\frac{1}{2}}}$$

$$du_3 = \frac{q_3 dx'}{4\pi [r^2 + (x-x')^2]^{\frac{3}{2}}}$$

Only the component in the x direction need be considered for elongated bodies and sections and so we have

$$dv_2 = \frac{q_2 (x-x') dx}{2\pi [y^2 + (x-x')^2]} \quad dv_3 = \frac{q_3 (x-x') dx}{4\pi [r^2 + (x-x')^2]^{\frac{3}{2}}}$$

The source and sink intensity q_2 and q_3 can be related to the ordinates y and r by means of the continuity law, that gives

$$q_2 = 2U_\infty dy/dx \quad q_3 = 2\pi V_\infty r \frac{dr}{dx}$$

$$\text{so } dv_2 = \frac{V_\infty}{\pi} \frac{(x-x')}{[y^2 + (x-x')^2]} \frac{dy}{dx} dx'$$

$$dv_3 = \frac{V_\infty}{2} \frac{(x-x')}{[r^2 + (x-x')^2]^{\frac{3}{2}}} r \frac{dr}{dx} dx'$$

If the same velocity gradient is desired in the body and in the section, the following relationship must exist between y and r .

$$\int \frac{1}{r} \left\{ \frac{(x-x')}{[y^2 + (x-x')^2]} \right\} \frac{dy}{dx} dx' = \int \frac{1}{2} \left\{ \frac{(x-x')}{[r^2 + (x-x')^2]^{\frac{3}{2}}} \right\} r \frac{dr}{dx} dx'$$

The solution of which results in a non-explicit expression involving log and arctg. of y and r .

An approximate and direct solution may be obtained, observing that the functions between brackets have a sharp maximum for $(x-x') = \pm y$ and $(x-x') = \pm \sqrt{2} r$, falling away for other values. Substituting $(x-x')$ by y and $\sqrt{2} r$ we obtain.

$$\frac{dr}{r} = \frac{3}{\pi} \frac{\sqrt{3}}{2} \frac{dy}{y}; \quad \log r = \frac{3}{\pi} \frac{\sqrt{3}}{2} \log y$$

and finally we have $r = y^{1.17}$.

A more correct solution would be obtained, using a $(x-x')$ corresponding to the bracketted function center of gravity, instead of that corresponding to its maximum.

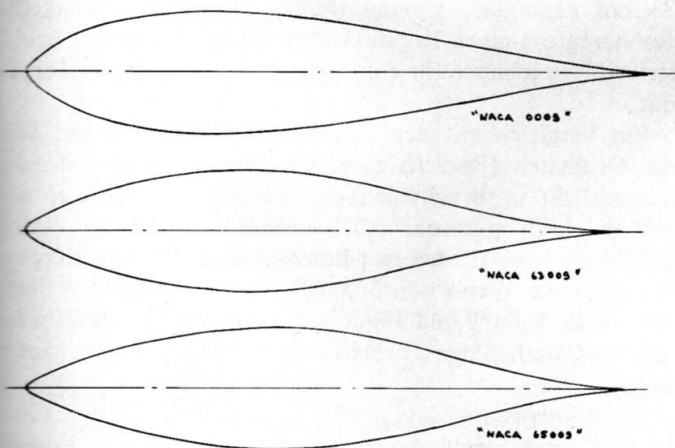


Fig. 4 - Contours of bodies derived from NACA airfoils 0009, 63009 and 65009

Such values being also functions of x' themselves, no direct relationship results, but analysing the two functions we see that if that were possible a larger exponent of y would result and an approximate "law" in the form:

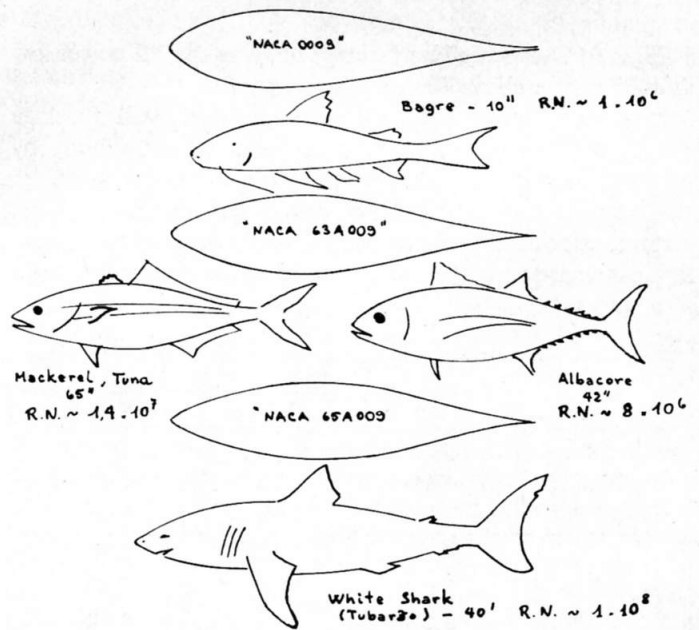
$$r = y^{2/3}$$

is now assumed.

4. The "fish" bodies

By means of the above expression the ordinates of three bodies, were computed from the NACA airfoils 0009, 63009 and 65009, the results being presented in table 1 and figure 4.

An amazing similarity is shown between the so calculated bodies and some fishes, as shown by figure 5 where the



Ref. 4

Fig. 5 - Comparison between the computed bodies derived from NACA airfoils and fishes

NACA 0009, 63A009 and 65A009 derived bodies, are compared with corresponding low medium and high Reynolds Numbers fishes. Although water is 800 times heavier than air, its kinematic viscosity is only 0,07 of that of air, and fish operating Reynolds Numbers fall within the operating range of gliders.

For instance a 45" tuna travelling at 19 knots and a 6 m glider fuselage flying at 60 mph. have the same Reynolds Numbers (~ 10 million).

5. Fuselage Design

In actual glider fuselage design, the "pure" low drag body of revolution is not practical and some modifications are needed to allow for the following design features.

- Pilot visibility and internal arrangement.
- Wing up down-wash for $C_L \neq 0$.
- Minimum cross section.
- Tail cone structural strength.
- Angle of attack range.

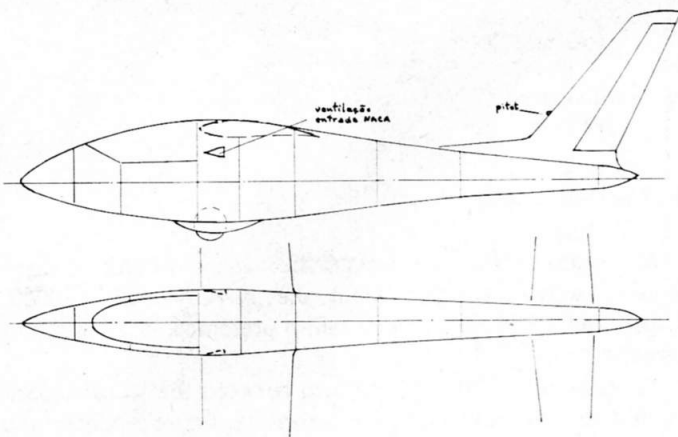


Fig. 6 – Example of «low drag» glider fuselage obeying the $3/2$ power law

Figure 6 shows a glider fuselage obeying the $3/2$ power law as well as the above design parameters.

It is now important to remember, that such fuselage shapes will only *favour* laminar flow in their forebody by creating favourable negative pressure gradients. Actually, this laminar flow will only be achieved if factors such as: surface smoothness and waviness, cabin sealing and ventilating etc., are carefully controlled resulting in an imprevi-

6. Conclusion

In the design of fuselages, tip tanks, propeller spinners, wheel fairings etc., pointed shaped bodies, with hyperbolic or parabolic noses may give less drag than rounded or elliptic-nosed shapes.

A simple and approximate method to obtain such shapes is to compute the $2/3$ power of tabulated airfoil coordinates.

Many existing gliders may obtain some “penetration” gains by means of a simple nose cone modification, accompanied by cabin sealing and surface finishing.

References

1. Schlichting/Trunckenbrodt—Aerodynamik des Flugzeuges, Springer Verlag, Berlin 1960.
2. Carl Kaplan—A new method for calculating potential flow past a body of revolution. NACA Report 752, 1942.
3. F. X. Wortmann—Widerstandsverminderung bei Segelflugzeugen, Aero-Revue, 12/1965.
4. Encyclopedia Britannica—Fishes.

Zusammenfassung der Arbeit von Galvao

Für dreidimensionale Körper (anders als für Flügelprofile) sind aerodynamische Werte kaum verfügbar; bei hohen Geschwindigkeiten ist jedoch der Rumpf von grosser Bedeutung.

Viele Segelflugzeuge haben Rumpfformen ähnlich denen von Flügelschnitten, doch zeigt schon die Potentialtheorie, dass verschiedene Ergebnisse mit derselben Form in zwei- und dreidimensionaler Strömung erhalten werden. Als Beispiel zeigt Figur 1 einen Vergleich der Strömung hinter einem Zylinder und einer Kugel. Die Methode von Quellen und Senken kann dazu benutzt werden, die Geschwindigkeitsverteilung um einen Rotationskörper zu berechnen; Figur 2 stellt die Ergebnisse für elliptische und parabolische Körper dar.

Ein Vergleich mit den obigen Methoden legt nahe, dass die Ordinaten (Radien) eines dreidimensionalen Körpers, ausgedrückt in Bruchteilen der maximalen Ordinate, ungefähr gleich sind der $3/2$ -Potenz der Ordinaten (halbe Dicke) des äquivalenten zweidimensionalen Körpers. Körper, die auf diese Weise von 3 NACA-Profilen abgeleitet sind, werden in Tafel 1 und Figur 4 dargestellt. Sie sind bemerkenswert ähnlich den Formen einiger Fische, wie in Figur 5 gezeigt.

Es ist interessant, dass die Reynolds-Zahlen für den Fisch und für einen Segelflugzeugrumpf ähnlich sind, weil Wasser – obwohl dichter als Luft – eine niedrigere kinematische Zähigkeit besitzt.

Ein Segelflugzeugrumpf, dessen Form ungefähr übereinstimmt mit oben angegebener $3/2$ -Potenz-Regel, ist in Figur 6 gezeigt.

Hans Zacher

Swiss Aero-Revue 1/1969

x	Ratio $r = y^{3/2}$		
	009	63009	65009
0	0	0	0
1,25	1,69	1,23	1,09
2,5	2,75	1,99	1,69
5	4,35	3,25	2,75
7,5	5,59	4,32	3,68
10	6,58	5,26	4,52
15	8,02	6,81	5,99
20	8,92	7,98	7,19
25	9,40	8,84	8,15
30	9,54	9,36	8,86
35	—	9,64	9,33
40	9,08	9,38	9,53
45	—	8,90	9,45
50	7,92	8,16	9,02
55	—	7,23	8,26
60	6,34	6,15	7,24
65	—	5,00	6,07
70	4,56	3,85	4,82
75	—	2,76	3,59
80	2,76	1,78	2,42
85	—	.98	1,41
90	1,13	.41	.63
95	.47	.09	.15
100	0	0	0

Table 1 – Coordinates of three bodies derived from NACA 0009, 63009 and 65009 airfoils

nose (see Wortmann's article in ref. 3). If not, as with wing sections, these shapes may give poorer results than obtained with more conventional fuselages.